# We are IntechOpen, the world's leading publisher of Open Access books Built by scientists, for scientists

6,900
Open access books available

185,000
International authors and editors

200M
Downloads

Our authors are among the

154
Countries delivered to

TOP 1%
most cited scientists

12.2%
Contributors from top 500 universities




WEB OF SCIENCE™

Selection of our books indexed in the Book Citation Index in Web of Science™ Core Collection (BKCI)

## Interested in publishing with us?
## Contact book.department@intechopen.com

Numbers displayed above are based on latest data collected.
For more information visit www.intechopen.com



Chapter

# Graphite Oxide: A Simple and Reproducible Synthesis Route

*Ernesto Hernández-Hernández, Perla J. Hernández-Belmares, Mónica A. Ceniceros-Reyes, Oliverio S. Rodríguez-Fernández and Pablo González-Morones*

## Abstract

The synthesis of graphite oxide (GrO) by oxidation of graphite has been carried out by different procedures. In this chapter, we describe a simple synthesis route based on Hummers' method without the usage of $NaNO_3$ achieving nearly the same outcomes, and this methodology is directed toward high-quality scale production of GrO with similar properties compared with GrO obtained with traditional and improved Hummers' methods. The GrO was obtained in a series of batch reactions and characterized by different techniques, and the results showed identical interlayer *d-space*, type and content of oxygen functionalities, and $I_D/I_G$ ratio. The high reproducibility of this methodology offers an efficient alternative for the large-scale production of graphene oxide.

**Keywords:** graphite oxide, graphene oxide, modified Hummers' method, reproducibility, oxidation process

## 1. Introduction

Graphenic materials have been one of the most studied materials in the history of humanity due to their outstanding properties such high thermal, electrical, mechanical, and permeability properties, among others [1]. For this reason, many potential applications have been proposed and demonstrated in scientific reports and patents. It has even been estimated that the global graphene market size will increase up to 38% from the years 2017 to 2025 [2], taking into an account its potential use in applications as automotive lightweight materials, aeronautics and energy, Li batteries, paints, functional coatings, solar cells, biosensors, membranes, and electronics, just to mention some of them [3–7]. One of the main technological challenges that engineers and scientific community face is the lack of new methods of large-scale production of graphene and its derivative. The graphite is inexpensive and available in large quantity and unfortunately does not readily exfoliate to yield individual graphene sheets. Graphite oxide (GrO) is a layered material produced by the oxidation of graphite. In contrast to pristine graphite, the GrO sheets, known as graphene oxide, are heavily oxygenated, bearing hydroxyl and epoxide functional groups on their basal planes, in addition to carbonyl and carboxyl groups presumable located at the sheet edges, nevertheless, there are certain features that still remain unknown among which stands out the chemical structure [8]. Particularly,

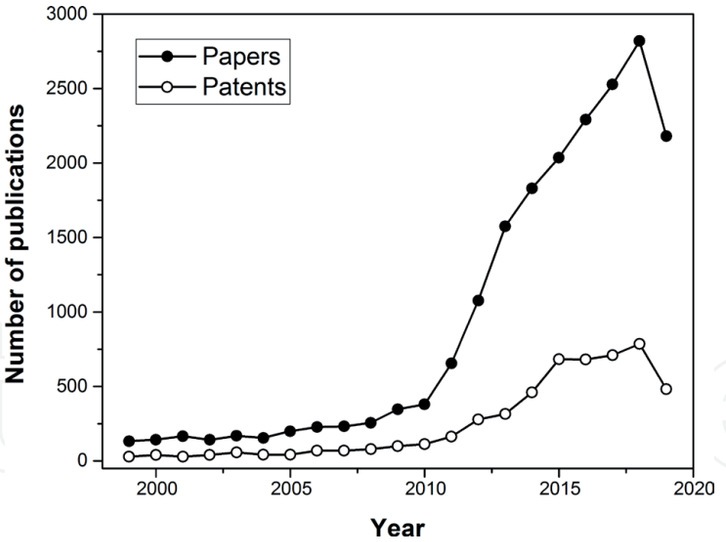



**Figure 1.**
*Number of scientific articles and patents published related to the synthesis of graphite oxide. Source: Data obtained by the analysis using SciFinder.*

graphene oxide (GO) has gained interest since it can be used for a wide scale of chemical transformations that include the reduction of graphene-like materials and its functionalization with other functional groups [9].

The number of publications in patents and research manuscripts related to the synthesis and production of graphite oxide and graphene oxide is shown in **Figure 1**. An abrupt increase in publications was observed after 2010. In 2018, approximately 2800 papers and 800 patents were published, and there is a tendency to increase the publications of both documents in the next years. This trend discloses the interest of these materials, which are expected to impact in the applications mentioned above.

The GrO can be prepared through several approaches, and each of them has their own advantages and flaws [10]. The main goal is to produce GrO at large scale with the best characteristics and high reproducibility; thus, the methodology here described consists in a variation of Hummers' method with important improvements that allow a successful synthesis of GrO.

## 2. Synthetic approaches

Graphene oxide can be synthesized via chemical oxidation of graphite, predominantly. Nevertheless, there are a few reports with an alternative electrochemical oxidation [11, 12]. Brodie's method, reported in 1859, was the first one in utilizing potassium chlorate to the mixture of graphite and nitric acid as the oxidant and intercalating agents, respectively. However, this technique has important flaws, such as the reaction time is about 4 days, low yield of the GO, the evolution of toxic acid vapors and $NO_2/N_2O_4$ gases, and the generation of highly explosive $ClO_2$ when chlorate mixed with strong acids [13]. Nearly 40 years later, Staudenmaier proposed the use of $H_2SO_4$ with $HNO_3$, but the explosive $ClO_2$ gas still remained as long as the prolonged reaction time. Based on Staudenmaier's work, Hummers and Offeman developed an alternative method that has been widely used for the synthesis of graphite oxide [14]. The chemicals used in this case were $H_2SO_4$ to intercalate graphite with the assistance of $NaNO_3$ and $KMnO_4$ as oxidant agents. The main reasons that this procedure is a reference in this matter are the use of $KMnO_4$ (strong oxidant) guarantees the completion of reaction within several hours, and the safety issue, in which there is no production of explosive $ClO_2$ due

to the absence of $KClO_3$, and there is no generation of acid fog due to the replacement of $HNO_3$ with $NaNO_3$. Despite of its high efficiency and the safety matter, it still has some drawbacks: (1) the toxic gas generation ($NO_2/N_2O_4$), (2) residual $Na^+$ and $NO_3^-$ ions are difficult to be removed after GrO synthesis and purification, and (3) incomplete oxidation resulting in the formation of graphite/GrO mixture [15, 16]. These problems have led to made several modifications to Hummers' method, and the main strategies includes the removal of $NaNO_3$. One of them is reported by Tour et al. [15] by increasing the amount of $KMnO_4$ and a 9:1 mixture of concentrated $H_2SO_4/H_3PO_4$ with a reaction time higher than 12 h. The GrO obtained by this methodology was highly oxidized with fewer defects in the basal plane and higher yield (77%), compared to GrO prepared by Hummers' method (40%). Shi et al. [16] removed the $NaNO_3$ from traditional Hummers method; with this simple modification, it was possible to produce GrO without affecting the yield and still had a high C/O ratio (2.36). Yu et al. [10] also reported a further improvement for $NaNO_3$-free Hummers' method by partly replacing $KMnO_4$ with $K_2FeO_4$; in addition, the amount of sulfuric acid was considerably reduced. This procedure resulted in a high yield (84%) compared to the Hummers traditional method.

The synthesis yield is normally estimated considering the mass ratio of graphite and graphite oxide. Methods aforementioned reported high yield by increasing the amount of oxidant agent and/or reaction time or by adding another reactant (acid or intercalating agent). These modifications may imply important disadvantages such as high cost, poor scalability, and practical applications. Based on $NaNO_3$-free Hummers' method, authors of the present chapter propose some changes in order to obtain oxidized sheets but keeping the graphenic properties and also to get these two themes in a scalable way. **Figure 2** illustrates the methodology in which the mixture of graphite-$H_2SO_4$ was previously sonicated to improve the intercalation of

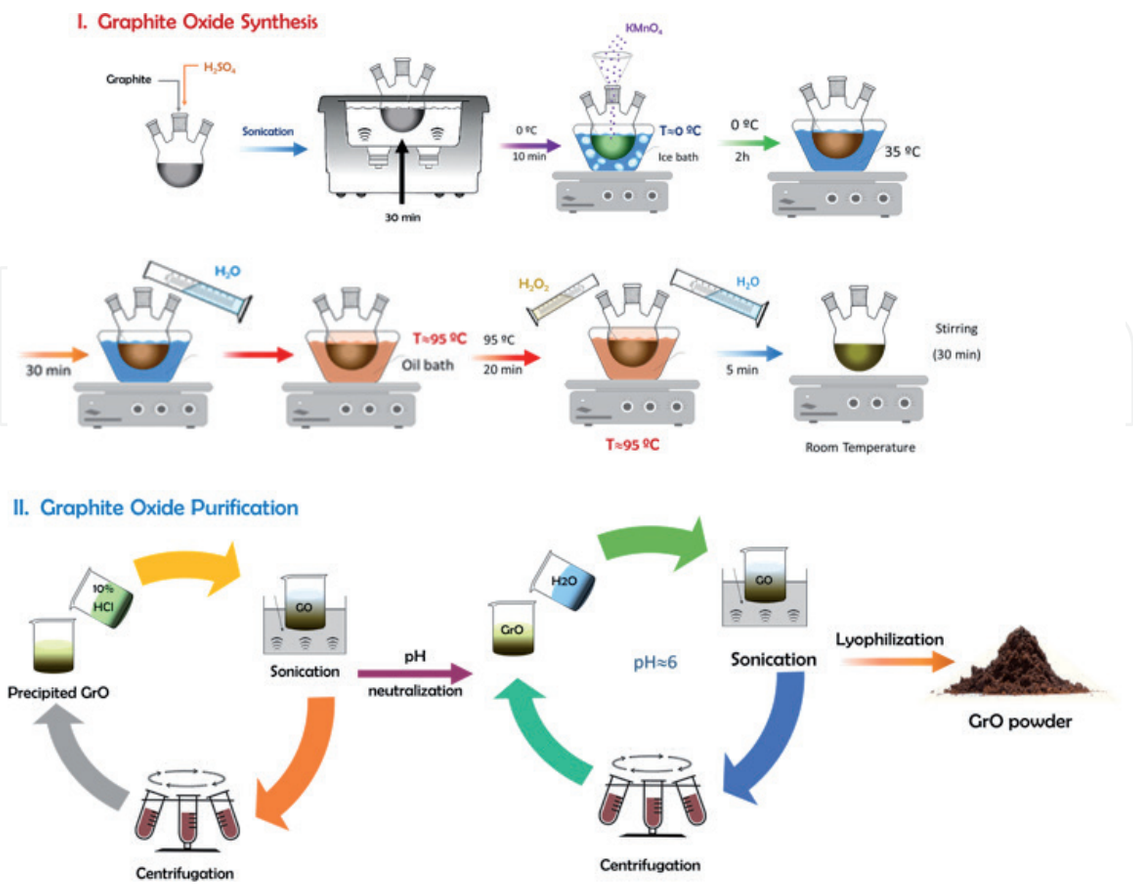



**Figure 2.**
*Scheme of GrO synthesis proposed by the authors based on $NaNO_3$-free Hummers' method.*

| Method | Graphite (g) | Oxidant | Graphite/oxidant ratio | Reaction time (h) | C/O atomic ratio | Yield of GrO (%) | Ref |
|---|---|---|---|---|---|---|---|
| Hummers | 100 | 300 g $KMnO_4$ + 50 g $NaNO_3$ | 1:3 | ~2 | 2.1–2.9 | 40 | [14] |
| Tour | 3 | 18 g $KMnO_4$ | 1:6 | >12 | — | 77 | [15] |
| Shi | 3 | 9 g $KMnO_4$ | 1:3 | ~2 | 2.36 | — | [16] |
| Zhang | 10 | 11 g $KMnO_4$ + 4 g $KFeO_4$ | 1:1.5 | 5 | 2.12 | 84 | [10] |
| Author's work | 2 | 6 g $KMnO_4$ | 1:3 | ~4 | 1.98–2.1 | 55 | [17] |

**Table 1.**
*Comparison among different methods to synthesize GrO.*

the acid between graphite galleries. Also, controlling the addition time of $KMnO_4$ ($t \leq 30$ min) and increasing the stirring time would enhance the diffusion of the $KMnO_4$ in the interlayer space. The obtained GrO in this procedure with the reaction time of 4 h has similar properties with those reported in the literature [17].

**Table 1** shows noteworthy aspects of different methods to produce GrO, with respect to the chemicals involved, reaction time, C/O atomic ratio, and yield. The most important thing is the fact that has been proven to be a promising scalable method for obtaining graphite oxide, which was possible to demonstrate with the final features studied from several GrO samples synthesized.

## 3. GrO properties

In order to evaluate the reproducibility of the method proposed by the authors of the present chapter, GrO was synthesized in a total of 10 batch reactions, and the graphite oxide obtained was labeled GrO 1, GrO 2, ..., GrO *n*, where *n* corresponds to the reaction number. All GrO *n* samples were characterized by different analytical techniques and were compared to each other, including the precursor graphite, labeled as GT. The structural, chemical, thermal, and morphological properties are presented below.

### 3.1 Structural properties

The samples were analyzed by XRD to evaluate the crystalline structure of GT and different synthesized GrO. **Figure 3** shows the comparison among GT and three of the GrO samples (GrO 3, GrO 4, and GrO 7). XRD pattern of GT shows a characteristic diffraction peak ($d_{002}$) at 26.5° that corresponds to a *d*-space of 0.33 nm. After oxidation, this peak is no longer observable, instead a broad peak at a range of 11.1–11.6° can be assigned to $d_{001}$, which oscillates from 0.76 to 0.79 nm, and this increase in *d* spacing is attributed to the intercalation of water molecules and to the presence of the functional groups at the basal plane [8, 18, 19]. The XRD experimental data of each sample are presented in **Table 2**, and it is observed that the average position peak of all GrOs at $2\theta = 11.37 \pm 0.18°$ has an average interlayer space $d_{001} = 0.78 \pm 0.1$ nm. The Full Width at Half Maximum (FWHM) was used to estimate the thickness, $L_c$, by the Scherrer equation [20], whose results vary between 9.97 and 15 nm. The thickness, $L_c$, was used to calculate the average number of

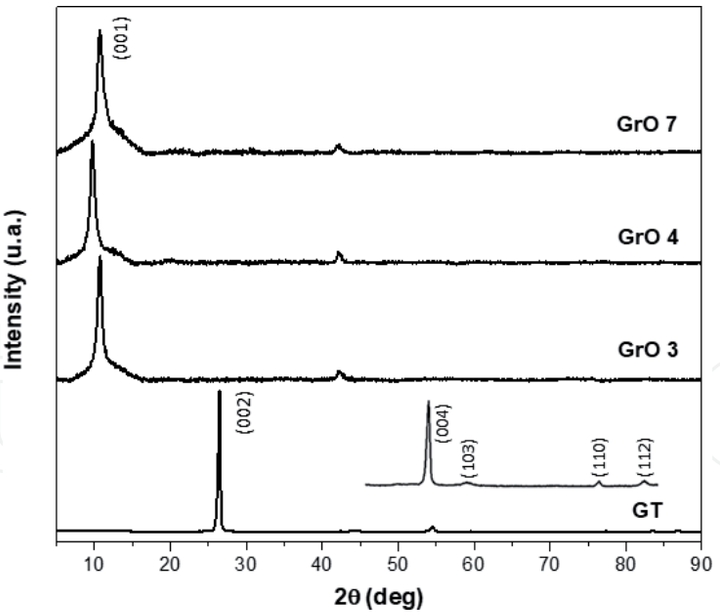



**Figure 3.**
*X-ray diffraction patterns of GT, GrO 3, GrO 4, and GrO 7 [17].*

| Sample | 2θ (°) | $d_{001}$ (nm) | FWHM (°) | Thickness (nm) | Number of layers (thickness/d) |
|---|---|---|---|---|---|
| GT | 26.50 | 0.34 | 0.32 | 25.17 | 74.90 |
| GrO 1 | 11.37 | 0.78 | 0.70 | 11.46 | 14.75 |
| GrO 2 | 11.43 | 0.77 | 0.55 | 14.54 | 18.81 |
| GrO 3 | 11.15 | 0.79 | 0.61 | 12.99 | 16.38 |
| GrO 4 | 11.27 | 0.78 | 0.53 | 15.00 | 19.12 |
| GrO 5 | 11.19 | 0.79 | 0.70 | 11.47 | 14.52 |
| GrO 6 | 11.15 | 0.79 | 0.61 | 13.09 | 16.50 |
| GrO 7 | 11.64 | 0.76 | 0.80 | 9.97 | 13.13 |
| GrO 8 | 11.61 | 0.76 | 0.59 | 13.44 | 17.66 |
| GrO 9 | 11.37 | 0.78 | 0.56 | 14.37 | 18.48 |
| GrO 10 | 11.49 | 0.77 | 0.61 | 13.19 | 17.15 |
| Average | 11.37 | 0.78 | 0.63 | 12.95 | 16.65 |
| Std. dev. | 0.18 | 0.01 | 0.08 | 1.58 | 2.00 |

**Table 2.**
*X-ray data comparison among different GrO samples.*

layers, being of 16.65 ± 2 for GrO, which is significantly low compared with the ~75 layers estimated for GT, and this indicates that periodic structure of graphite has been disrupt, and it has partially exfoliated forming small stacks of few layers.

The structural changes caused by oxidation process were also monitored by Raman spectroscopy. The Raman spectra of GT and GrO 2, GrO 4, and GrO 6 are compared in **Figure 4**. The GT exhibits a sharp and strong G band at around 1580 $cm^{-1}$, associated with bond stretching of the $sp^2$ carbon pairs in both rings and chains, and a weak and broad D band at 1350 $cm^{-1}$, associated with the presence of defects in graphite materials such as bond-angle disorder, bond-length disorder, vacancies, and etch defects [21]. The blue shift of the G band and the significantly

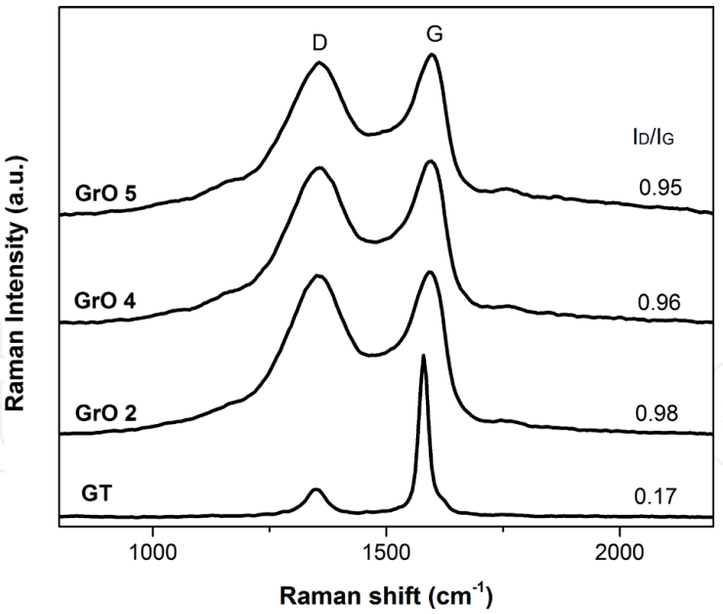



**Figure 4.**
*Raman spectra of GT, GrO 2, GrO 4, and GrO 5 [17].*

| Sample | D band | | | G band | | | $I_D/I_G$ | La (nm) |
|---|---|---|---|---|---|---|---|---|
| | FWHM | Position ($cm^{-1}$) | Raman intensity | FWHM | Position ($cm^{-1}$) | Raman intensity | | |
| GT | 57.75 | 1350.63 | 0.17 | 24.39 | 1579.25 | 1.00 | 0.17 | 110.14 |
| GrO 1 | 199.13 | 1362.50 | 0.98 | 174.08 | 1596.59 | 1.00 | 0.98 | 19.67 |
| GrO 2 | 188.79 | 1350.63 | 0.98 | 135.81 | 1590.81 | 1.00 | 0.98 | 19.65 |
| GrO 3 | 195.98 | 1356.57 | 0.95 | 153.29 | 1596.59 | 1.00 | 0.95 | 20.27 |
| GrO 4 | 206.51 | 1356.57 | 0.96 | 153.24 | 1596.59 | 1.00 | 0.96 | 20.04 |
| GrO 5 | 191.20 | 1356.57 | 0.95 | 172.73 | 1596.59 | 1.00 | 0.95 | 20.25 |
| GrO 6 | 190.69 | 1356.57 | 0.99 | 178.67 | 1596.59 | 1.00 | 0.99 | 19.41 |
| GrO 7 | 144.54 | 1348.20 | 0.80 | 93.17 | 1588.67 | 0.86 | 0.94 | 20.53 |
| GrO 8 | 163.68 | 1348.20 | 0.80 | 101.67 | 1588.67 | 0.86 | 0.93 | 20.67 |
| GrO 9 | 173.00 | 1360.09 | 0.90 | 113.99 | 1594.45 | 0.93 | 0.96 | 19.98 |
| GrO 10 | 169.57 | 1360.09 | 0.896 | 126.74 | 1600.23 | 0.946 | 0.95 | 20.29 |
| | | | | | | Average | 0.96 | 20.08 |
| | | | | | | Std. dev. | 0.02 | 0.41 |

**Table 3.**
*Analysis of results obtained by Raman spectroscopy for GT and all GrO samples.*

increase in the width and intensity of D band for all GrO samples with respect to GT can be associated with the defects induced in the hexagonal carbon network by the formation of oxygen functionalities and the parallel incorporation of $sp^3$ bonds during the oxidation of graphite (see **Table 3**). In addition, the notable increase in the intensity ratio $I_D/I_G$ from 0.17 for GT to 0.96 ± 0.02 for GrO reveals a drastic decrease in the size of carbon $sp^2$ domains [22, 23] and can be corroborated by calculating the crystallite size, La, which is considerably less for GrO (~20 nm) than GT (110 nm) [24].

### 3.2 Thermal properties

Thermal stability of all GrO samples was evaluated by TGA, and some of them are presented in **Figure 5a** and were compared with GT that remains thermally stable to a temperature of above 700°C, whereas the thermal degradation of GrO presents several weight losses, the first at around 10% below 100°C is associated with the vaporization of adsorbed water molecules onto GO sheets, and the second weight loss of 30% is observed from 150 to 280°C, which is attributed to the thermal decomposition of labile oxygen functionalities, and it is also observed a small weight loss (~10%) from 270°C to 600°C, which is attributed to the removal of more thermally stable oxygen functional groups such as carbonyl groups [21, 25, 26]. The derivative weight loss curve of GrO presented in **Figure 5b** displays a maximum at 217–220°C related to the degradation of functional groups, and **Table 4** presents the weight loss at this temperature for all samples, whose average value is 30% with a degradation temperature of 218°C.

### 3.3 Chemical characterization

The FTIR and XPS analysis reveal significant chemical changes of GrO samples owing to oxidation process. FT-IR spectra in **Figure 6** compare results from GrO 6, GrO 7, and GrO 8 with GT. In all cases, GrO exhibited a broad peak at 3000–3700 $cm^{-1}$, which is attributed to O—H stretch vibration of hydroxyl, carboxyl, and intercalated free water. The vibrational peak at 1725 $cm^{-1}$ is associated with the C═O stretch of both carboxyl and carbonyl groups, and the vibrational peak at 1623 $cm^{-1}$ is assigned to the overlapped frequencies of bending modes of trapped water molecules and C═C stretch of unoxidized $sp^2$ carbon domains [27]. The O—H deformations of the C—OH groups appear at 1400 $cm^{-1}$. The peaks at 1220 $cm^{-1}$ and 1057 $cm^{-1}$ are associated with C—O stretching of epoxy and alkoxy groups, respectively [28].

On the other hand, the elemental chemical information of GrO 2 and GrO 7 samples was obtained by XPS analysis. The XPS survey spectra presented in **Figure 7** show the C 1s peak at 284.4 eV and O 1s peak at 533.5 eV, with an atomic content of oxygen of 34.6% and 32.1% for GrO 2 and GrO 7, respectively, being similar to that calculated by TGA. The atomic ratio C/O was 1.89 for GrO 2 and 2.08 for GrO 7, and these values coincide with those obtained for different GrOs synthesized by other techniques, as described in **Table 1**.

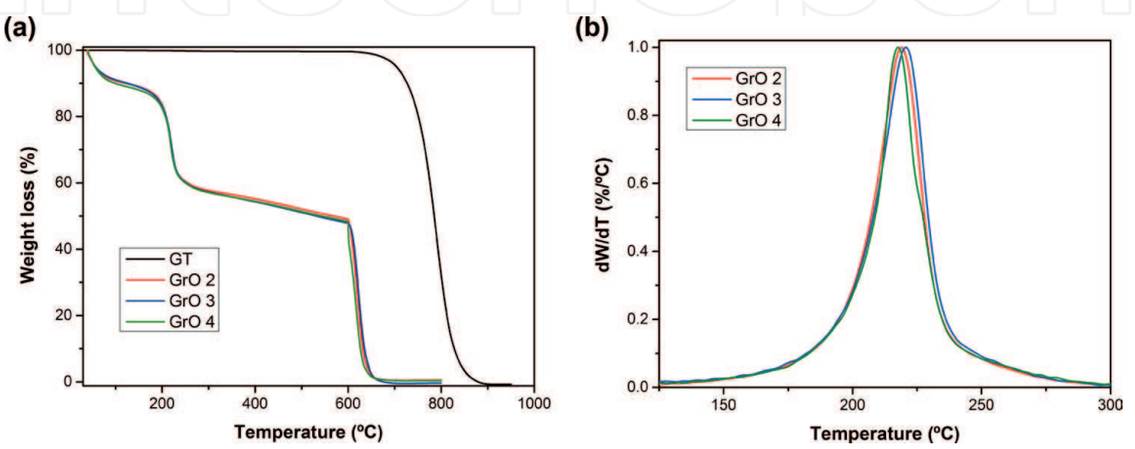



**Figure 5.**
*Thermal behavior of GT and GrO: (a) TGA curves and (b) dW/dT curves of GT, GrO 2, GrO 3, and GrO 4 [17].*

| Sample | % Weight loss at 150–280°C | $T_{max}$ (°C) |
|---|---|---|
| GrO 1 | 28.77 | 219.86 |
| GrO 2 | 30.06 | 218.94 |
| GrO 3 | 30.91 | 220.63 |
| GrO 4 | 29.64 | 217.15 |
| GrO 5 | 28.05 | 217.09 |
| GrO 6 | 30.3 | 217.03 |
| GrO 7 | 29.62 | 220.28 |
| GrO 8 | 31.49 | 218.76 |
| GrO 9 | 31.86 | 214.87 |
| GrO 10 | 30.00 | 217.12 |
| Average | 30.07 | 218.17 |
| Std. dev. | 1.16 | 1.82 |

**Table 4.**
*TGA data of all GrO samples.*

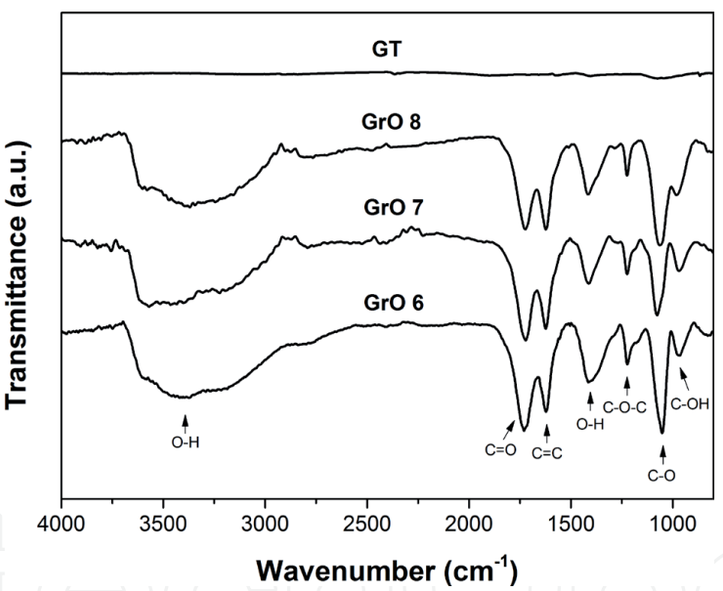



**Figure 6.**
*FT-IR spectra of GT, GrO 6, GrO 7, and GrO 8 [17].*

High-resolution XPS spectra of GrO in the C 1s region, shown in **Figure 8**, present the signals corresponding to nonoxygenated carbon rings (C═C/C—C, 284.7 eV), hydroxyl (C—OH, 286.3 eV), epoxy (C—O—C, 286.9 eV), carbonyl (C═O, 287.4 eV), and carboxyl groups (O═C—OH, 289.4 eV), which are consistent with the signals of the FT-IR spectra [16, 17, 23, 29].

Owing to the fact that several factors such as the nonstoichiometry nature of GrO, the size of the sheets, and no-homogeneity distribution of functional groups over the sheets and the fact that XPS is a technique of surface analysis, the concentration of oxygen functionalities among the specimens is not 100% reproducible, which has been consistent with previous reports; nevertheless, through other analysis techniques, it is demonstrated that the procedure for obtaining GrO is reproducible.

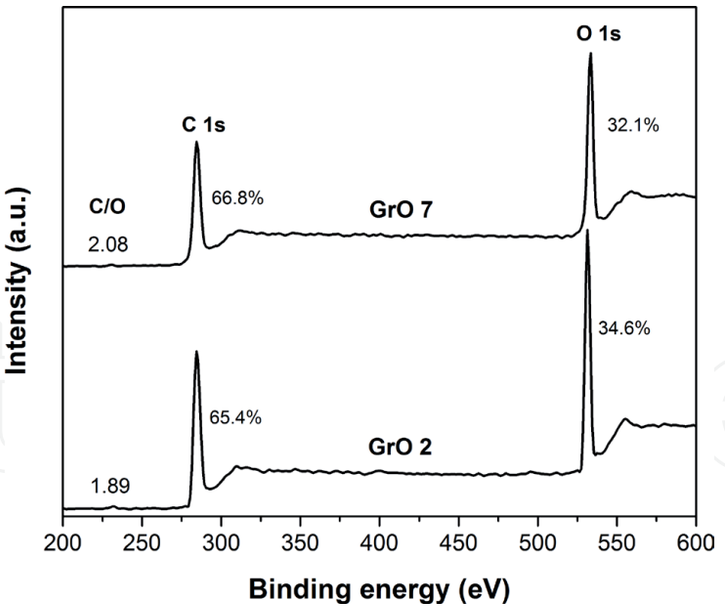



**Figure 7.**
*XPS general survey of GrO 2 and GrO 7 [17].*

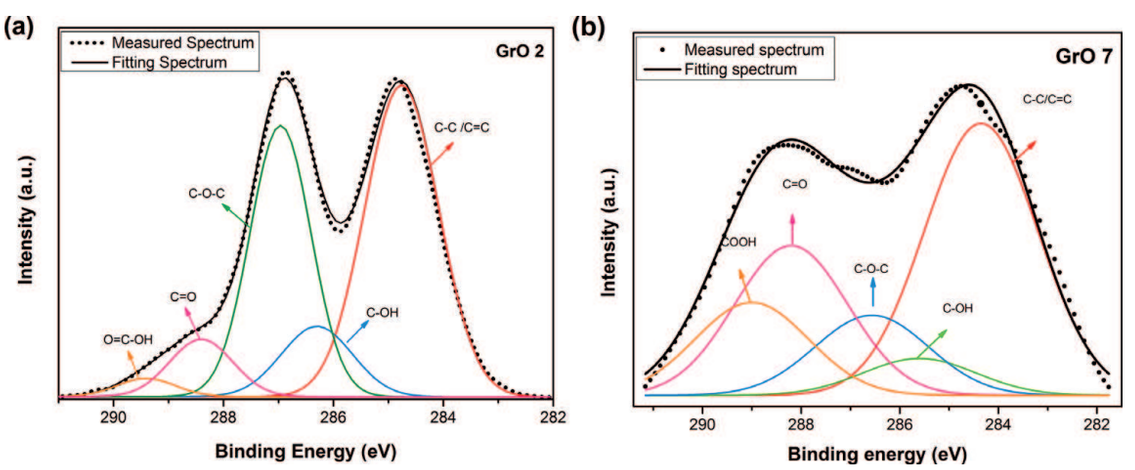



**Figure 8.**
*HR-XPS survey spectrum of (a) GrO 2 and (b) GrO 7 [17].*

## 3.4 Morphological properties

GrO powders were exfoliated in aqueous media via ultrasonic vibration, since it is one of the most common methods to exfoliate graphene oxide sheets [8], and the obtained samples were analyzed by TEM and AFM to monitor the morphology and the structure. The nanosheets and pure GT as well were studied by TEM in conventional mode (CTEM) and selected area electron diffraction mode (SAED), and **Figure 9a** shows a general view of GT, and it is clearly observed the plate-like shape, the borders are shown with different contrast, caused most likely for the presence of several plates randomly accommodated, which is not the case of graphene oxide, and these sheets tend to wrinkle and fold [30] and have a "silky" appearance. SAED pattern of GT (inset in **Figure 9a**) confirmed the polycrystalline nature of graphite, and the incident beam is surrounded for several rings with distinctive diffraction dots that correspond with some of its crystallographic planes, such as (201), (110), (100) and (101), according with the diffraction card: *PDF Card No.: 00-001-0646.*

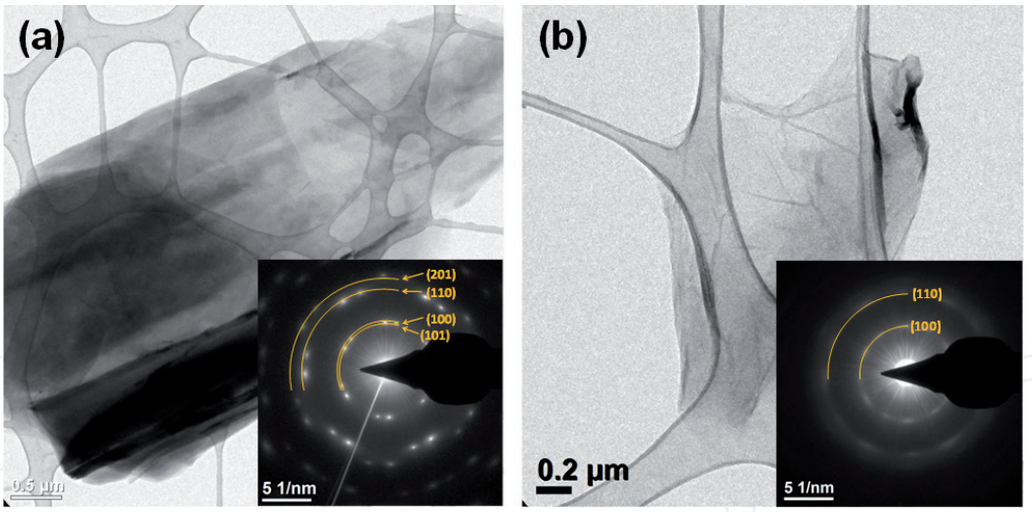



**Figure 9.**
*TEM images of (a) GT and (b) GO, both with inset SAED showing the assigned planes [17].*

The SAED pattern of GO (inset in **Figure 9b**) confirmed the disordered nature and shows a diffraction rings that are not well defined and unresolved dots, which is consistent with amorphous materials. Nevertheless, the measurements of these rings confirm the planes (100) and (110), which suggest the presence of regions with graphitic nature [23].

Atomic force microscopy (AFM) analysis was carried out to verify the number of layers of graphene oxide. The sample is collected from the dispersion prepared in deionized water, and this demonstrates that sonication promotes near-complete exfoliation of the GO; **Figure 10** exhibits an example of GO sheets with an estimated number of ~4 layers. Numerous nanosheets were detected in tapping mode, and the thickness profile showed around 1.45–6.42 nm, taking into consideration the *d*-space and the individual graphene sheet thickness (0.34 nm), leading to a conclusion that it was obtained GO with 1–6 layers, approximately [31].

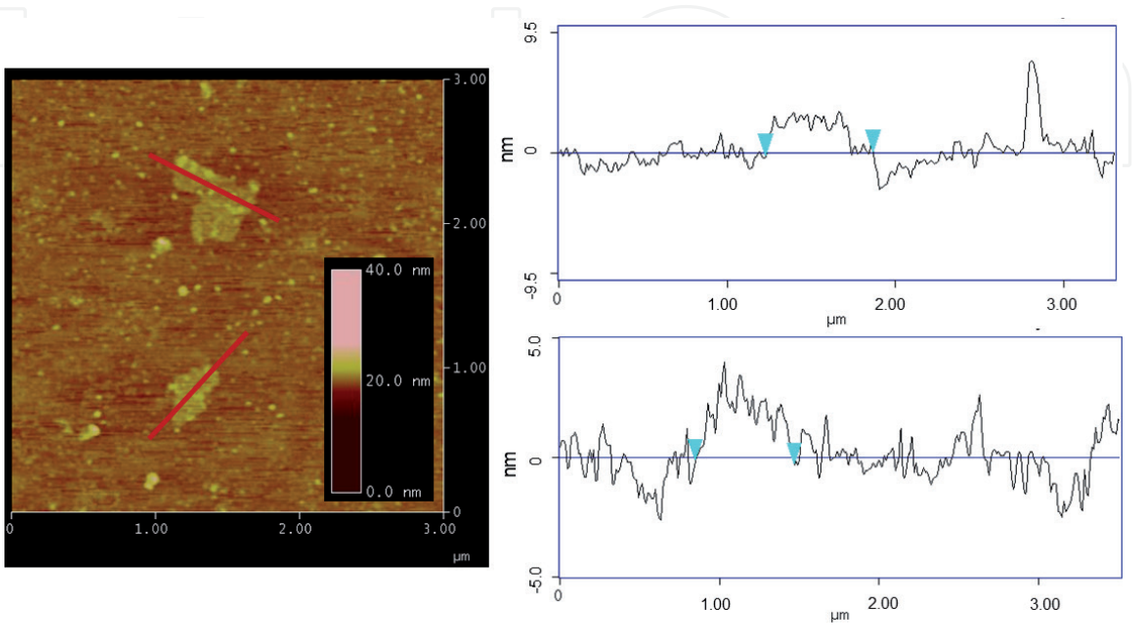



**Figure 10.**
*Tapping mode AFM view of GO nanosheets with their thickness profile [17].*

## 4. Conclusions

In summary, the protocol used to synthesize GrO based on Hummers' modified method proved to be a successful procedure. As has been demonstrated in early reports, the use of $NaNO_3$ is not a variable that influences the final product, and it is possible to achieve GrO with similar properties and characteristics by using a simple, small reaction time and more safe methodology. Besides the removal of $NaNO_3$, changes such as (a) enabling the sonication of graphite with sulfuric acid, (b) the slow addition of $KMnO_4$, and (c) the two-hour stirring of the mixture $KMnO_4$/graphite/sulfuric acid at 0°C were key factors that contributed to ensure reproducibility. This affirmation was supported by several analyses carried out to the 10 GrO samples synthesized. Oxygen functionality content, determined by TGA and XPS, was estimated of ~30 and ~33%, respectively; the type of these functional groups was identify by FTIR and corresponds to carboxyl, carbonyl, epoxy, and hydroxyl groups. Raman confirms that the layers of GrO have $sp^2/sp^3$ domains, suggesting that even though the oxidation has occurred, the sheets still possess graphenic characteristics; analyses performed by TEM pointed out that since SAED results showed graphenic ordering. This means that the material has the advantages of having functional groups in order to accomplish important chemical reactions (functionalization and reduction) while still possessing graphenic properties.

This proposed method can be used to synthesize GrO and other graphenic materials in an economical and large-scale way.

## Acknowledgements

The support of the CONACYT through Grant 299,092 (LANIAUTO) is greatly appreciated. Also, the authors are grateful to Dr. Roberto Yañez Macías, Dr. Carlos Gallardo Vega, and Dr. Enrique Díaz Barriga Castro for their technical support.

## Author details

Ernesto Hernández-Hernández*, Perla J. Hernández-Belmares, Mónica A. Ceniceros-Reyes, Oliverio S. Rodríguez-Fernández and Pablo González-Morones
Departamento de Materiales Avanzados, Centro de Investigación en Química Aplicada (CIQA), Saltillo, Coahuila, Mexico

*Address all correspondence to: ernesto.hernandez@ciqa.edu.mx

IntechOpen

© 2019 The Author(s). Licensee IntechOpen. This chapter is distributed under the terms of the Creative Commons Attribution License (http://creativecommons.org/licenses/by/3.0), which permits unrestricted use, distribution, and reproduction in any medium, provided the original work is properly cited. CC BY

## References

[1] Huang X, Yin Z, Wu S, et al. Graphene-based materials: Synthesis, characterization, properties, and applications. Small. 2011;**7**(14): 1876-1902. DOI: 10.1002/smll.201002009

[2] Graphene Market Size, Share & Trends Analysis Report by Application (Electronics, Composites, Energy), by Product (Graphene Nanoplatelets, Graphene Oxide), by Region, and Segment Forecasts, 2019-2025. 2019

[3] Elmarakbi A, Azoti WL. Novel composite materials for automotive applications: Concepts and challenges for energy-efficient and safe vehicles. In: 10th International Conference on Composites Science and Technology. 2015

[4] Lawal AT. Biosensors and bioelectronics Progress in utilisation of graphene for electrochemical biosensors. Biosensors & Bioelectronics. 2018;**106**(2018):149-178. DOI: 10.1016/j.bios.2018.01.030

[5] Sharma N, Sharma V, Jain Y, et al. Synthesis and characterization of graphene oxide (GO) and reduced graphene oxide (rGO) for gas sensing application. Macromolecular Symposia. 2017;**1**(376):1-5. DOI: 10.1002/masy.201700006

[6] Chen K, Wang Q, Niu Z, Chen J. Graphene-based materials for flexible energy storage devices. Journal of Energy Chemistry. 2018;**27**:12-24. DOI: 10.1016/j.jechem.2017.08.015

[7] Bai L, Zhang Y, Tong W, et al. Graphene for energy storage and conversion: Synthesis and interdisciplinary applications. Electrochemical Energy Reviews. 2019:1-36. DOI: 10.1007/s41918-019-00042-6

[8] Dreyer DR, Park S, Bielawski CW, Ruoff RS. The chemistry of graphene oxide. Chemical Society Reviews. 2010;**39**:228-240. DOI: 10.1039/b917103g

[9] Kuila T, Bose S, Kumar A, Khanra P, Kim NH, Joong Hee L. Chemical functionalization of graphene and its applications. Progress in Materials Science. 2012;**57**(7):1061-1105. DOI: 10.1016/j.pmatsci.2012.03.002

[10] Yu H, Zhang B, Bulin C, Li R, Xing R. High-efficient synthesis of graphene oxide based on improved Hummers method. Scientific Reports. 2016;**6**:36143. DOI: 10.1038/srep36143

[11] You X, Chang J-H, Ju BK, Pak JJ. An electrochemical route to graphene oxide. Journal of Nanoscience and Nanotechnology. 2011;**11**:5965-5968. DOI: 10.1166/jnn.2011.4451

[12] Pei S, Wei Q, Huang K, Cheng H, Ren W. Green synthesis of graphene oxide by seconds timescale water electrolytic oxidation. Nature Communications. 2018;**9**(145):1-9. DOI: 10.1038/s41467-017-02479-z

[13] Chen J, Li Y, Huang L, Li C, Shi G. High-yield preparation of graphene oxide from small graphite flakes via an improved Hummers method with a simple purification process. Carbon N Y. 2015;**81**:826-834. DOI: 10.1016/j.carbon.2014.10.033

[14] Hummers WJ, Offeman RE. Preparation of graphitic oxide. Journal of the American Chemical Society. 1958;**89**(9):1339. DOI: 10.1021/ja01539a017

[15] Marcano DC, Kosynkin DV, Berlin JM, et al. Improved synthesis of graphene oxide. ACS Nano.

2010;**4**(8):4806-4814. DOI: 10.1021/nn1006368

[16] Chen J, Yao B, Li C, Shi G. An improved Hummers method for eco-friendly synthesis of graphene oxide. Carbon N Y. 2013;**64**(1):225-229. DOI: 10.1016/j.carbon.2013.07.055

[17] Hernández BP, Rodriguez FO, Hernández HE. Elaboración de nanocompuestos de PA6/óxido de grafeno en el estado fundido, mediante el uso del concentrado PA6/rGO y de suspensions GO-$H_2O$ [Tesis doctoral en proceso]. CIQA: Programa de Doctorado en Tecnología de Polímeros; 2016

[18] Lerf A, Buchsteiner A, Pieper J, et al. Hydration behavior and dynamics of water molecules in graphite oxide. Journal of Physics and Chemistry of Solids. 2006;**67**:1106-1110. DOI: 10.1016/j.jpcs.2006.01.031

[19] Buchsteiner A, Lerf A, Pieper J. Water dynamics in graphite oxide investigated with neutron scattering. The Journal of Physical Chemistry. B. 2006;**110**: 22328-22338

[20] Saenko NS. The X-ray diffraction study of three-dimensional disordered network of nanographites: Experiment and theory. Physics Procedia. 2012;**23**:102-105. DOI: 10.1016/j.phpro.2012.01.026

[21] Wang H, Hu YH. Effect of oxygen content on structures of graphite oxides. Industrial and Engineering Chemistry Research. 2011;**50**:6132-6137. DOI: 10.1021/ie102572q

[22] Yang D, Velamakanni A, Park S, et al. Chemical analysis of graphene oxide films after heat and chemical treatments by X-ray photoelectron and Micro-Raman spectroscopy. Carbon N Y. 2009;**47**:145-152. DOI: 10.1016/j.carbon.2008.09.045

[23] Krishnamoorthy K, Veerapandian M, Yun K, Kim SJ. The chemical and structural analysis of graphene oxide with different degrees of oxidation. Carbon N Y. 2013;**53**:38-49. DOI: 10.1016/j.carbon.2012.10.013

[24] Pimenta MA, Dresselhaus G, Dresselhaus MS, Cancado LG, Jorio A, Saito R. Studying disorder in graphite-based systems by Raman spectroscopy. Physical Chemistry Chemical Physics. 2007;**9**:1276-1291. DOI: 10.1039/b613962k

[25] Shen J, Hu Y, Shi M, et al. Fast and facile preparation of graphene oxide and reduced graphene oxide nanoplatelets. Chemistry of Materials. 2009;**21**(15):3514-3520. DOI: 10.1021/cm901247t

[26] Chu H, Lee C, Tai N. Green reduction of graphene oxide by *Hibiscus sabdariffa* L. to fabricate flexible graphene electrode. Carbon N Y. 2014;**80**:725-733. DOI: 10.1016/j.carbon.2014.09.019

[27] Acik M, Lee G, Mattevi C, et al. The role of oxygen during thermal reduction of graphene oxide studied by infrared absorption spectroscopy. Journal of Physical Chemistry C. 2011;**115**: 19761-19781. DOI: 10.1021/jp2052618

[28] Rattana T, Chaiyakun S, Witit-Anun N, et al. Preparation and characterization of graphene oxide nanosheets. Procedia Engineering. 2012;**32**:759-764. DOI: 10.1016/j.proeng.2012.02.009

[29] Yuan R, Yuan J, Wu Y, Chen L, Zhou H, Chen J. Efficient synthesis of graphene oxide and the mechanisms of oxidation and exfoliation. Applied Surface Science. 2017;**416**:868-877. DOI: 10.1016/j.apsusc.2017.04.181

[30] Pandey DK, Fung T, Prakash G, Piner R, Chen YP, Reifenberger R. Surface science folding and cracking of

graphene oxide sheets upon deposition. Surface Science. 2011;**605**:1669-1675. DOI: 10.1016/j.susc.2011.04.034

[31] Frankberg EJ, George L, Efimov A, Honkanen M, Pessi J, Levänen E. Measuring synthesis yield in graphene oxide synthesis by modified Hummers method. Fullerenes, Nanotubes, and Carbon Nanostructures. 2015;**23**(9):755-759. DOI: 10.1080/1536383X.2014.993754

IntechOpen

IntechOpen